Supplementary Materials

Our traction cytometry method is consistent with Newtonian mechanics

In our experiments, the cells are submerged in buffer and crawl on a substrate. At any time during migration, the product of cell mass and acceleration (inertia) must be equal to the difference between the forward traction force produced by the cell and the viscous drag exerted by the surrounding fluid. From our shape and velocity measurements, we estimated that the magnitude of the inertial effects and the viscous drag forces over the cell are always very small, and of the order of 0.1 pico Newtons (Del Alamo et al., 2007). Therefore, the cells in our experiments must exert a non-zero but very small net force on the substrate while moving. Previous methods developed by others were designed to yield a zero net traction forces regardless of the actual measurements (Butler et al., 2002; Dembo et al., 1996). These methods are based on the Boussinesq solution of the elastostatic equation, which assumes an infinitely thick gel. Our method takes the finite thickness of the substrate into account, which enables the determination of these non-zero net traction forces. The net force exerted by a cell on an elastic substrate of Young modulus E, Poisson ratio σ and thickness h is

$$\vec{F}_{net} = \int\int \left[\tau_{xz}(x,y), \tau_{yz}(x,y)\right] dxdy = \frac{E}{2(1+\sigma)h} \int\int \vec{u}(x,y) dxdy, \qquad \text{(S1)}$$

where $\vec{u}(x,y)$ is the horizontal vector deformation field measured at the surface of the substrate and $\vec{\tau}(x,y) = [\tau_{xz}(x,y),\ \tau_{yz}(x,y)]$ are the stress (force/area) exerted by the cell on the substrate. Figure S1 shows histograms of the net traction force's magnitude measured for all cells studied, as well histograms of the ratio between the net traction force and the average magnitude of the force exerted by the cell at each location, which was defined as

$$F_R = \int\int \sqrt{\tau_{xz}^2(x,y) + \tau_{yz}^2(x,y)}\, dxdy. \qquad \text{(S2)}$$

Table S1 shows the average and standard deviation of $|F_{net}|$ and $|F_{net}/F_R|$ for the three cell lines used in this study. The results indicate that the measured net forces are approximately 10 pN, which is rather small if one considers that a single myosin II head can generate a force stroke of about 5 pN (Finer et al., 1994). Figure S1 and Table S1 also show that the measured net forces are between 50 and 100 times smaller than the average magnitude of the contractile forces exerted by the cell, which is within the error of our measurements. The discrepancy between the measured net forces and our theoretical estimations of 0.1 pN (Del Alamo et al., 2007) may either be due to the simplified assumptions used for the estimation of the drag or be due to experimental noise. In summary, the net traction forces we measure and our estimates are consistent with Newton's second law of mechanics.

Selection of threshold for separating motility cycle into stages has negligible effect on phase-averaged traction maps

We separated and sorted the different stages of the motility cycle by dividing each cycle of the time evolution of cell length, L(t), into the phases during which it is increasing (phase 1, protrusion), is near a local maximum (phase 2, contraction), is decreasing (phase 3, retraction), or is near a local minimum (phase 4, relaxation). This algorithm applies a threshold on L(t) as shown in equation 7 of the main article text, which depends on a threshold parameter, α, that can vary between 0 and 0.5. Figures 3, 5, and 6 in the manuscript were plotted using $\alpha = 0.2$. To check whether our results are independent of α, we re-calculated figure 5 for values of the threshold parameter lower and higher than $\alpha = 0.2$. The resulting stress maps shown in Figures S2 and S3 respectively are highly similar to those in Figure 5, confirming that our results are robust irrespective of the threshold.

Some traction stresses are expected to fall outside the average cell shape contour in our phase averages

Figure 5 shows non-zero average traction forces outside of the average cell contours. *A priori*, this result may appear counter-intuitive because the cell can only apply traction forces inside its two-dimensional outline at

each instant of time. However, as discussed in the Materials and Methods, when one plots the averaged distribution of traction forces superposed on the averaged cell contour the variability in cell shape leads to non-zero average forces outside of the average cell contour. This effect is illustrated in Figure S6, which shows the average force map obtained from the three snapshots shown in Figure S4. This figure shows that the solid black lines, which represent the instantaneous cell contours, extend beyond the dashed blue contour that represents the average cell contour at some locations. This explains why we should not expect the average traction stresses to be constrained to the inside of the average cell contour.

In contrast to the methods of others (Butler et al., 2002; Dembo et al., 1996), our method does not constrain the stresses to the cell outline and a small proportion of the stresses we calculate for individual cells are localized outside their contour. We therefore want to show that even we when eliminate this small contribution, the statistical variability of cell shape alone leads to non-zero traction stresses outside of the average cell contour. For that purpose, we re-calculated the average traction stress map of Figure S4 using the constrained Fourier transform traction cytometry method proposed by Butler *et al*. (Butler et al., 2002). This method iteratively solves the elastostatic equation for the substrate and corrects the measured deformations to yield zero traction stresses outside of the cell upon convergence. Figures S7 and S8 are obtained with the constrained method and are equivalent to Figures S4 and S6. By the design of the constrained method, the obtained stresses are generally inconsistent with the experimentally measured deformation field (Dembo et al., 1996), and are known to be sensitive to small errors in the identification of the cell contour (Tolic-Norrelykke et al., 2002). Additionally, methods that constrain the forces outside the cell to zero, can lead to artificially elevated stresses near the cell's periphery. Despite these caveats, the stress fields shown in these plots are qualitatively similar. As expected, in the three snapshots of Figure S7 the traction stresses are zero outside of the instantaneous cell contour. However, the averaged traction stress map of these three cells in Figure S8 shows non-zero stresses in some locations outside of the average cell contour because there is a non-zero proportion of the cell outlines outside the average contour generating these stresses.

REFERENCES

Butler, J.P., I.M. Tolic-Norrelykke, B. Fabry, and J.J. Fredberg. 2002. Traction fields, moments, and strain energy that cells exert on their surroundings. *Am J Physiol Cell Physiol*. 282:C595-605.

Del Alamo, J., R. Meili, B. Alonso-Latorre, J. Rodriguez-Rodriguez, A. Aliseda, R. Firtel, and J. Lasheras. 2007. Spatio-temporal analysis of eukaryotic cell motility by improved force cytometry. *Proc Natl Acad Sci U S A*. 104:13343-8.

Dembo, M., T. Oliver, A. Ishihara, and K. Jacobson. 1996. Imaging the traction stresses exerted by locomoting cells with the elastic substratum method. *Biophys J*. 70:2008-22.

Finer, J.T., R.M. Simmons, and J.A. Spudich. 1994. Single myosin molecule mechanics: piconewton forces and nanometre steps. *Nature*. 368:113-9.

Tolic-Norrelykke, I.M., J.P. Butler, J. Chen, and N. Wang. 2002. Spatial and temporal traction response in human airway smooth muscle cells. *Am J Physiol Cell Physiol*. 283:C1254-66.

SUPPLEMENTARY TABLE AND FIGURE LEGENDS

Table S1

The magnitude of net traction is negligible. The left column contains the net forces measured in pico Newtons (F_{net}, see equation S1). The right column contains the ratio between the net forces and the average magnitude of the forces exerted by the cell at different locations, F_{net} / F_R (for a mathematical definition of F_R, see equation S2). Histograms of the instantaneous values of the magnitudes represented in this table are shown in figure S1.

Figure S1

Histograms of the net forces measured for all cells studied. Panels **(a)**, **(c)** and **(e)** show histograms of the net forces measured in pico Newtons (F_{net}, see equation S1). Panels **(b)**, **(d)** and **(f)** show histograms of ratio between the net forces and the average magnitude of the forces exerted by the cell at different locations, F_{net} / F_R (for a mathematical definition of F_R, see equation S4). Panels **(a)** and **(b)** correspond to WT cells. Panels **(c)** and **(d)** correspond to mlcE$^-$ cells. Panels **(e)** and **(f)** correspond to mhcA$^-$ cells. The averages and standard deviations corresponding to each of the histograms of this figure are shown in table S1.

Figure S2

Spatiotemporal mapping of the traction stresses exerted by wild-type and MyoII mutant cells showing phase-averaged traction stresses and cell shape corresponding to the 4 stereotypical stages defined in Figure 3. This figure is similar to Figure 5A but in this case the stages have been separated using a value of the threshold $\alpha = 0.14$ in Equation 7, instead of the value $\alpha = 0.2$ used in Figure 5.

Figure S3

Spatiotemporal mapping of the traction stresses exerted by wild-type and MyoII mutant cells showing phase-averaged traction stresses and cell shape corresponding to the 4 stereotypical stages defined in Figure 3. This

figure is similar to Figure 5A but in this case the stages have been separated using a value of the threshold α = 0.33 in Equation 7, instead of the value α = 0.2 used in Figure 5.

Figure S4.

Steps taken in the calculation of the average distribution of traction forces. **(a)** Snapshots (three) of the trajectory of a wild-type cell in the laboratory reference frame. The black contours are the measured cell outlines. The color shades and arrows indicate the magnitude and direction of the traction stresses exerted by the cell on the substrate. The dashed red lines represent the major and minor axes of the 2D projection of the cell (outline of the cell). The blue line represents the trajectory of the centroid of the cell. **(b-d)** Same three snapshots aligned and scaled into cell-based coordinates (eq. 9). The cells have been aligned so that their major axes always coincide with the x-axis, and their dimensions scaled with the length of the each cell. The dashed black line in these panels represents the average contour of WT cells. The labels "F" and "B" indicate respectively the front and back of the cell.

Figure S5.

(a) Two-dimensional contour map of the probability $\langle P(\xi,\eta)\rangle_i^N$ that a point belongs inside a wild-type cell in cell-based coordinates (eq. 9) for N = 31 cells and $i = 1$ (protrusion phase). The dashed lines represent the probability levels 0% and 95%. The solid line represents the probability level that encloses an area equal to the average area of wild-type cells during the protrusion stage, which in this case is Pav_i^N = 41%. Because it conserves the average area of the population, this contour has been chosen as the average outline of the cell. The labels "F" and "B" indicate respectively the front and back of the cell. **(b)** Three-dimensional representation of the probability map shown in **(a)**. The arrows shown at zero level indicate the magnitude and direction of the average traction forces and have been included for reference.

Figure S6

Average map of traction force resulting from the three snapshots shown in Figure S4. The solid black lines are the instantaneous cell contours coming from these three snapshots and the dashed blue contour is the average cell contour for WT cells. The labels “F” and “B” indicate respectively the front and back of the cell. Note that, because the instantaneous cell contours may exceed the average cell contour at some locations, the average traction stresses are not necessarily zero outside of the average cell contour.

Figure S7.

Same as figure S4 when the traction forces are calculated using the constrained iterative method proposed by Butler et al. (Butler et al., 2002) ,which imposes the forces to be zero outside of the instantaneous cell outline.

Figure S8.

Same as figure S6 when the traction forces are calculated using the constrained iterative method proposed by Butler et al. (Butler et al., 2002),which imposes the forces to be zero outside of the instantaneous cell outline. Note that, because the instantaneous cell contours may exceed the average cell contour at some locations, the average traction stresses are not zero outside of the average cell contour, even if the traction forces are always equal zero outside of the instantaneous cell contour (see Figure S7b-d).

Supplementary Movies

Movie M1

Animation of the phase averaged motility cycle of wild-type Dictyostelium discoideum cells. The animations of phase-averaged traction stresses (top) and cell area gain/loss measurements (bottom) illustrate the existence of a motility cycle with four canonical stages: protrusion, contraction, retraction, and relaxation. The magnitude and direction of the phase-averaged traction forces are indicated by color contours and arrows. Area gain/loss is indicated by red/blue color.

Movie M2

Animation of the phase averaged motility cycle of myosin essential light chain null Dictyostelium discoideum cells. The animations of phase-averaged traction stresses (top) and cell area gain/loss measurements (bottom) illustrate the existence of a motility cycle with four canonical stages: protrusion, contraction, retraction, and relaxation. The magnitude and direction of the phase-averaged traction forces are indicated by color contours and arrows. Area gain/loss is indicated by red/blue color.

Movie M3

Animation of the phase averaged motility cycle of myosin heavy chain null Dictyostelium discoideum cells. The animations of phase-averaged traction stresses (top) and cell area gain/loss measurements (bottom) illustrate the existence of a motility cycle with four canonical stages: protrusion, contraction, retraction, and relaxation. The magnitude and direction of the phase-averaged traction forces are indicated by color contours and arrows. Area gain/loss is indicated by red/blue color.

Table S1

		$\|F_{Net}\|$ (pN)	$\|F_{Net}/F_R\|$ (%)
wt	mean	7.70	1.62
	std	4.51	1.19
mlcE-	mean	11.29	2.03
	std	7.48	0.93
mhcA-	mean	10.39	1.85
	std	9.36	1.14

Figure S1

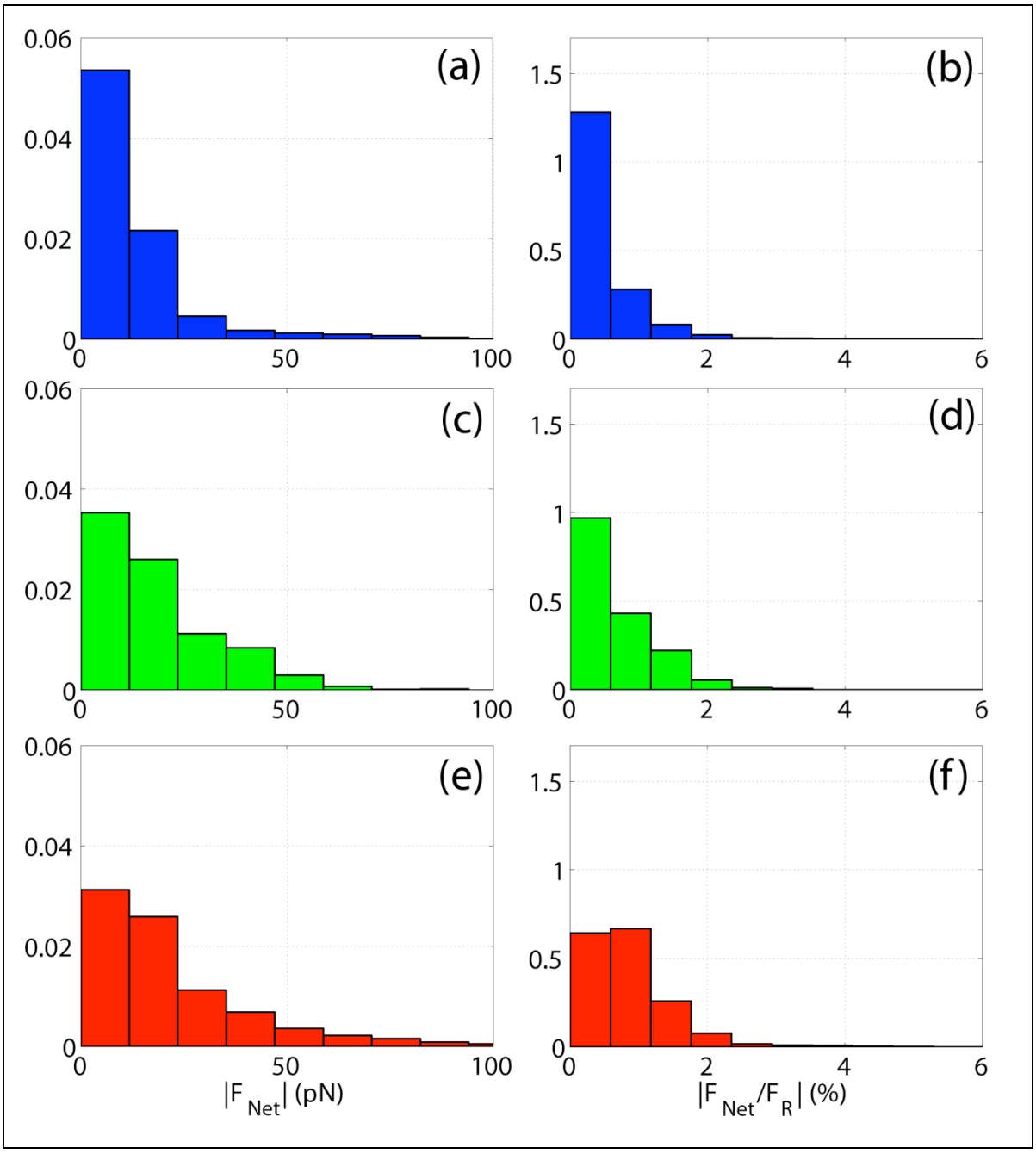

Figure S2

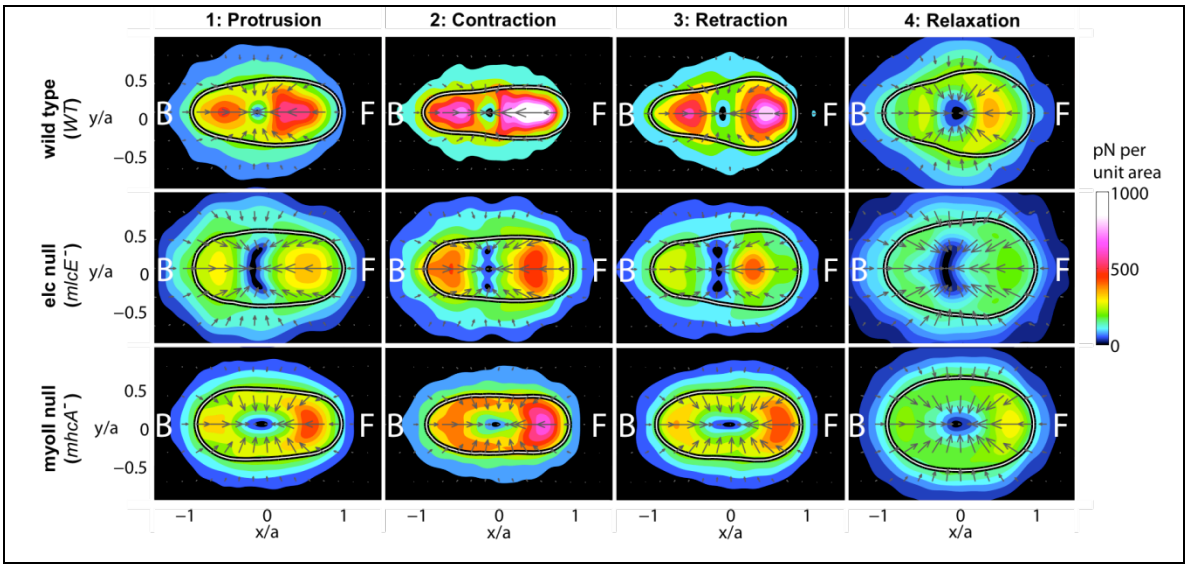
1: Protrusion
2: Contraction
3: Retraction
4: Relaxation
wild type (WT)
elc null (mlcE⁻)
myoII null (mhcA⁻)
y/a
0.5
0
−0.5
B
F
−1
0
1
x/a
pN per unit area
1000
500
0

Figure S3

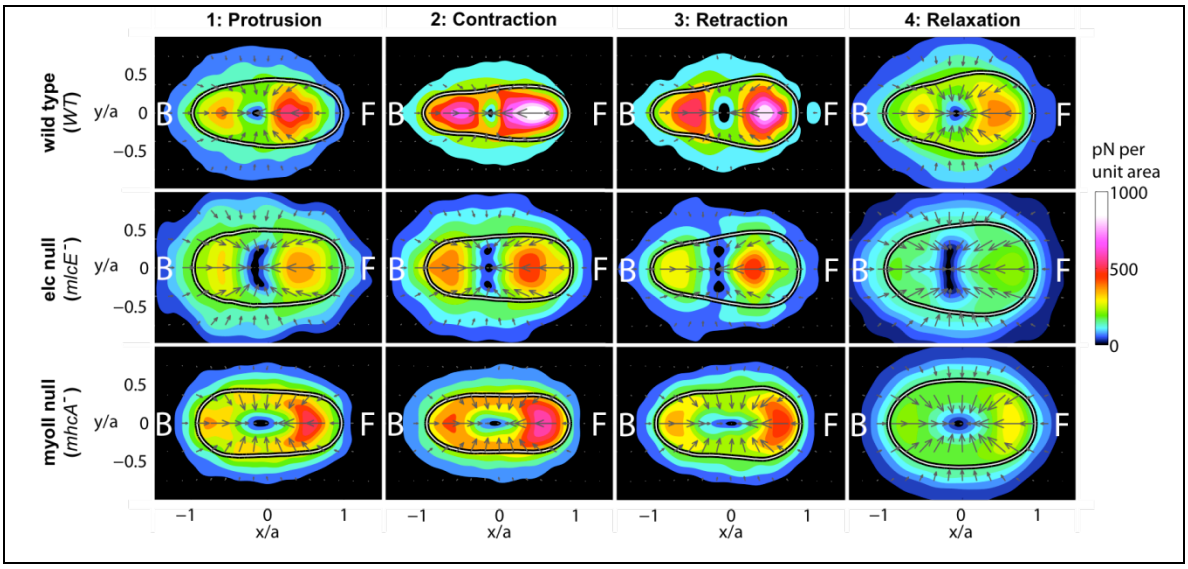
1: Protrusion
2: Contraction
3: Retraction
4: Relaxation
wild type (WT)
elc null (mlcE⁻)
myoII null (mhcA⁻)
y/a
0.5
0
−0.5
B
F
−1
0
1
x/a
pN per unit area
1000
500
0

Figure S4

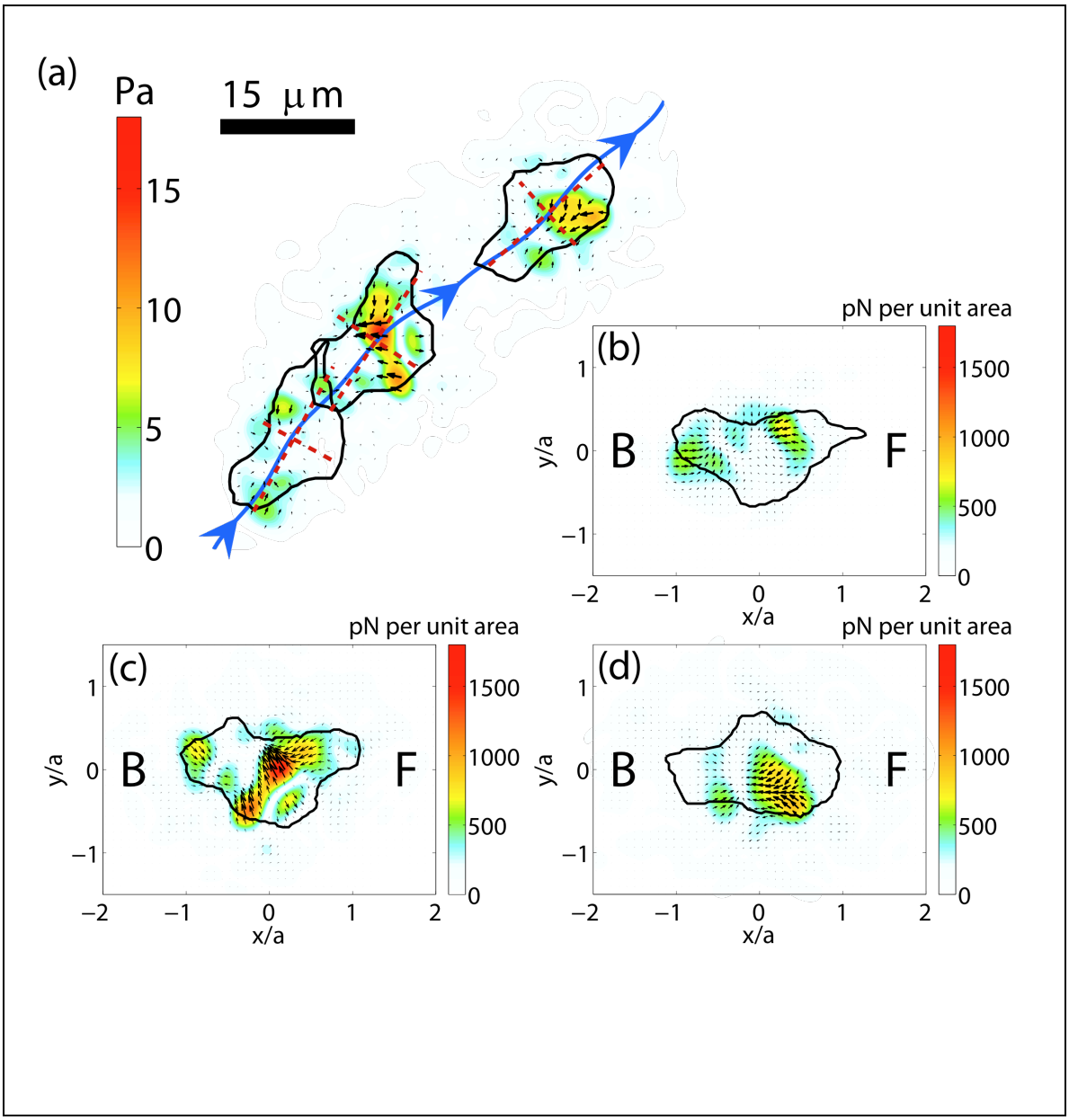

Figure S5

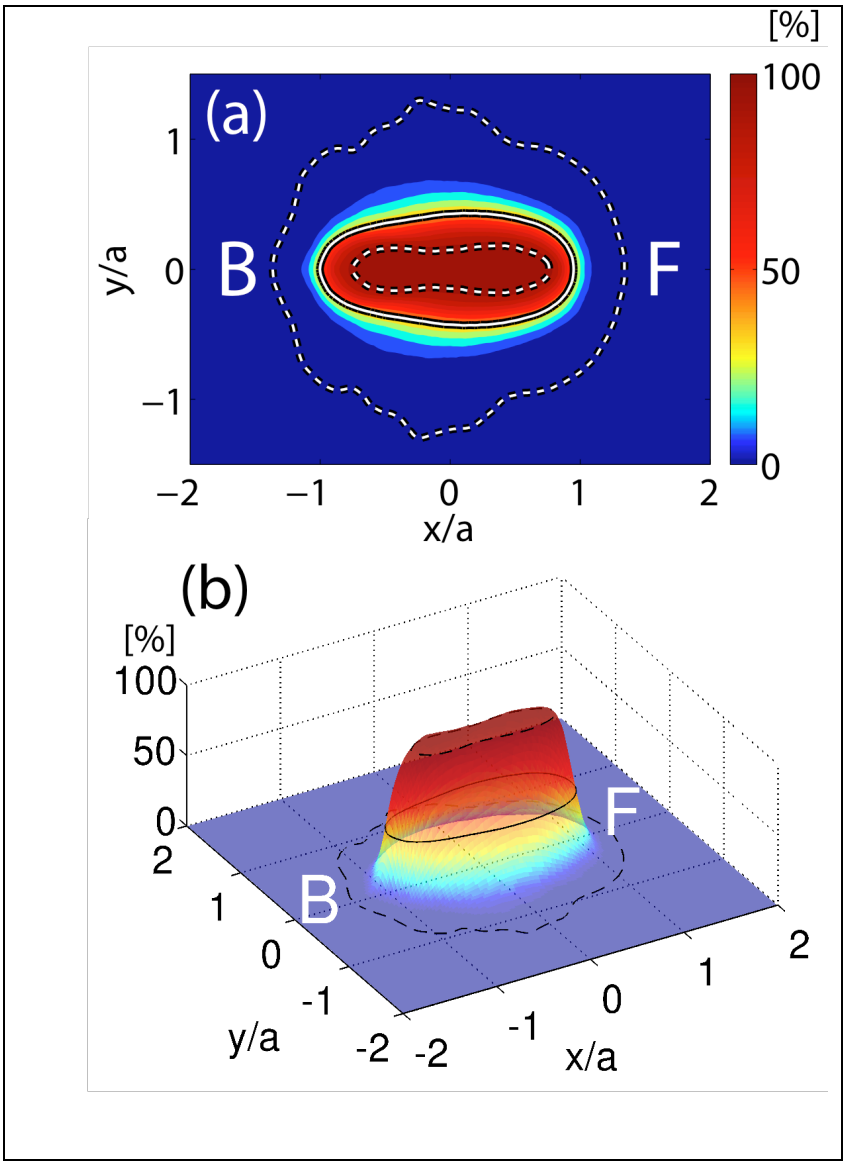

Figure S6

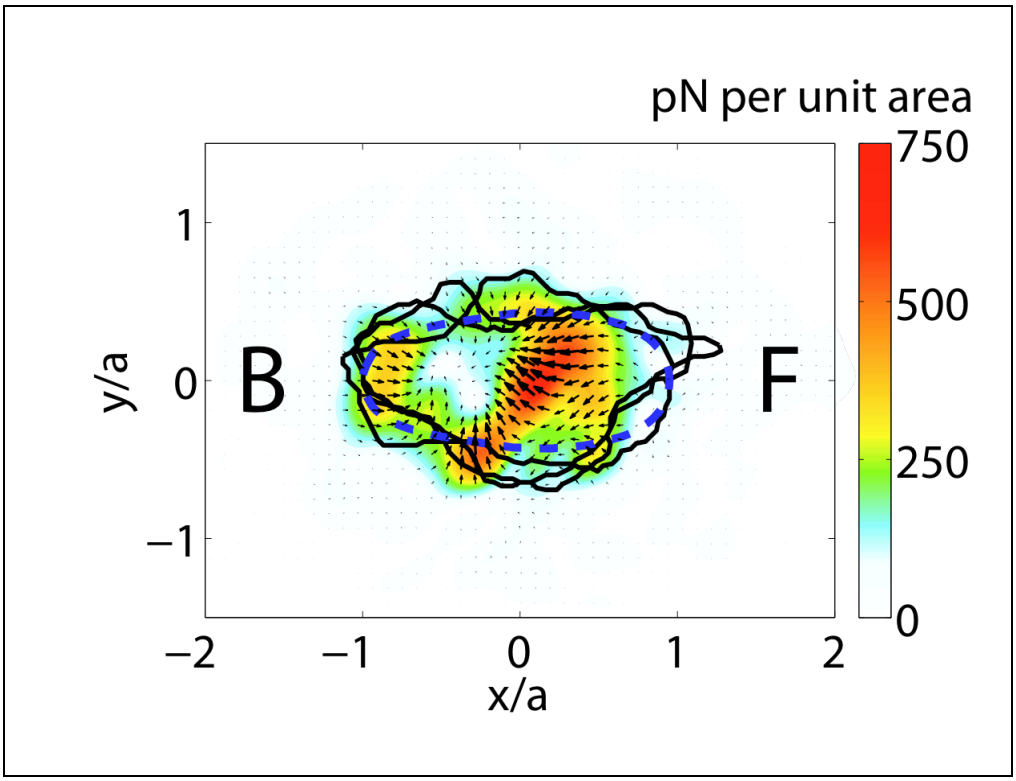

Figure S7

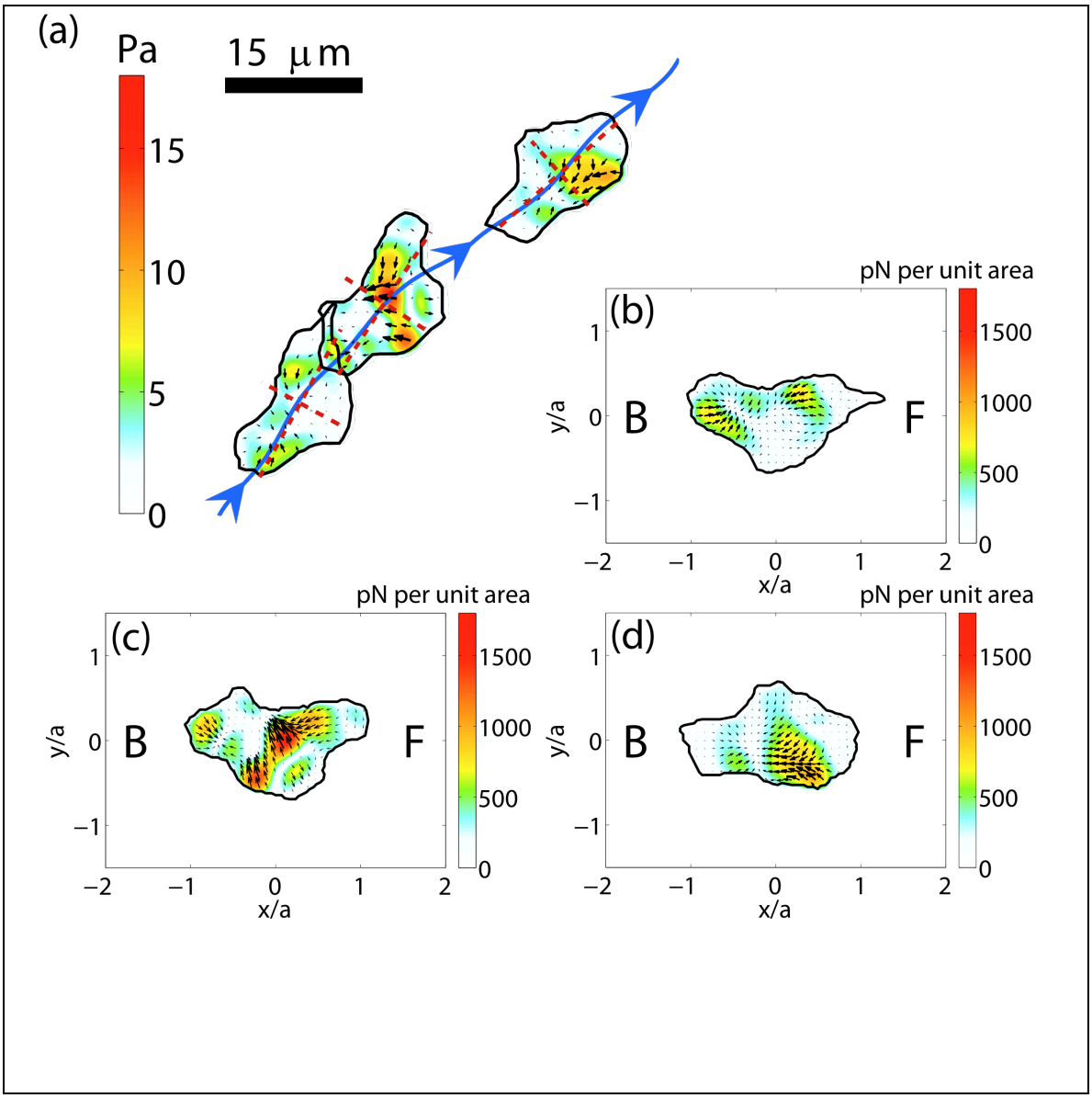

Figure S8